University of Baghdad
College of Engineering
JE
JOURNAL OF ENGINEERING

Journal of Engineering
journal homepage: www.joe.uobaghdad.edu.iq
Number 7 Volume 25 July 2019

Mechanical and Energy Engineering

An experimental and numerical investigation of heat transfer effect on cyclic fatigue of gas turbine blade

Abdullah Abdalrazaq Asaad *
M.Sc Candidate
Engineering College-
University of Baghdad
Abdullah.eng1990@gmail.com

Munther A. Mussa
Asst. Prof. Dr.
Engineering College-
University of Baghdad
Munthermech@yahoo.com

ABSTRACT

Blades of gas turbine are usually suffered from high thermal cyclic load which leads to crack initiated and then crack growth and finally failure. The high thermal cyclic load is usually coming from high temperature, high pressure, start-up, shut-down and load change. An experimental and numerical analysis was carried out on the real blade and model of blade to simulate the real condition in gas turbine. The pressure, temperature distribution, stress intensity factor and the thermal stress in model of blade have been investigated numerically using ANSYS V.17 software. The experimental works were carried out using a particular designed and manufactured rig to simulate the real condition that blade suffers from. A new controlled method in this rig was suggested to heating the specimen depending on Oxygen-gas flame. The numerical result shows that the temperature distribution over the blade varying with the load change, which leads to increase the stress intensity factor along the crack. The experimental result indicates that the rate of crack propagation varying with the position of crack and with the angle of inclined. Based on this result, more effective cracks on the blade were satisfied which are highly effect the blade lifetime.

Key words: gas turbine blade, turbine inlet temperature (TIT), thermal cyclic, crack propagation

فحص نظري وعملي لبيان تأثير انتقال الحرارة على الأجهاد الدوري في ريشة التوربين الغازي

الخلاصة

تعاني ريش التوربينات الغازية من حمل حراري دوري عالي يؤدي الى حدوث تشققات وبعدها نمو هذه الشقوق وبالتالي الفشل. هذا الحمل الحراري الدوري العالي يأتي من درجات الحرارة العالية، الضغط العالي، تشغيل المحرك التوربيني، أطفاء المحرك وتغيير الحمل. التحليلات العددية والاختبارات العملية انجزت على ريشة توربين حقيقية ونموذج لريشة التوربين لمحاكاة الظروف الحقيقية في التوربين الغازي. تم فحص الضغط، الحرارة، الاجهاد الحراري و معامل تركز الاجهادات على نموذج الريشة عدديا بواسطة برنامج ANSYS V.17 تمت الاختبارات العملية باستخدام جهاز مصمم ومصنع خصيصا لهذه الدراسة لمحاكاة الظروف الحقيقية التي تعاني منها الريشة في التوربين الغازي. في هذا الجهاز تم استخدام طريقة جديدة

*Corresponding author
Peer review under the responsibility of University of Baghdad.
https://doi.org/10.31026/j.eng.2019.07.04
2520-3339 © 2019 University of Baghdad. Production and hosting by Journal of Engineering.
This is an open access article under the CC BY-NC license http://creativecommons.org/licenses/by-nc/4.0/).
Article received: 6/5/2018
Article accepted: 25/6/2019

مسيطر عليها لتسخين العينة بالاعتماد على شعلة الاوكسجين-غاز. بينت النتائج العددية، ان توزيع درجات الحرارة في الريشة تتغير مع تغير الحمل والتي تؤدي الى زيادة معامل تركز الاجهاد على طول الشق. بينما بينت النتائج العملية ان معدل سرعة نمو الشق تتغير مع موقع الشق و زاوية ميل الشق على سطح الريشة. بالأعتماد على هذه النتائج تم تحديد الشق الأكثر تأثيرا على العمر الأفتراضي للريشة التوربينية.

1. INTRODUCTION

Gas turbines are one of the essential engines uses different fuels to produce mechanical energy. Most of gas turbine engine powers' are used to derive an electrical generator for electricity purpose or to drive fan for thrust purpose in ships and aircrafts. The turbine blade component plays important rule to take-out energy from high temperature and high pressure gases coming from combustion chamber. Therefore, it works under aggressive environment condition **Veeraragavan, 2012**. During repeated start-up, shut-down and load change operation the blade subjected to cyclic thermal which produced by quick gas temperature change and cyclic mechanical which produce by pressure difference and centrifugal force. This varying operation cycle is inducing under transient thermal and mechanical load called thermal – mechanical fatigue (TMF) or multiaxial fatigue. This cyclic cause complex microstructural damage which leads to crack initiation in the blade and finally failure , **Zhuang and Swansson, 1998**. Therefore, expecting the life of a turbine blade under (TMF) loading is very crucial and important in aeronautical engineering and gas turbine for the electrical purpose. In ,**Park, et al., 2002.** investigated the failure in (J69- T -25) turbojet engine blade and improved the safety of aircraft. Visual and surface examination showed that crack initiated and blade damage as a result of thermal air flow., **Jiang, 2003.** has examined the failure in gas turbine blade and noted that the failure as a result of low cycle fatigue is related to thermal stress caused by temperature gradient in short time period. ,**Bhaumik, et al., 2006.** investigated the failure of turbine blade in aero engine manufactured from Ni-base super alloy (CM 247 LC) which is worked at high temperature. Several examinations were carried out to study the details of crack in different blade to know the cause, orientation, length and depth of the crack. In the most examination, fatigue crack was obtained above blade root adjacent trailing edge.**Kim, 2009,** investigate fatigue of blade in aero engine. The (MAR200HF) blade was made of solidified nickel base super alloy and noted that crack initiated from trailing edge and propagate to the entire surface. At last, he found that the crack initiated as a result of pores in trailing edge and then propagate in surface blade as a result of cyclic load during service. **Jacobsson, 2004.** have experimentally inspected the specimen of nickel (Inconel 718) which is considers the base material for gas turbine blade under thermo-mechanical fatigue. They tried to evaluate the velocity of crack propagation to construct life model. **Wang, et al., 2013.** used an experimental and numerical method to obtained fatigue failure in mortise turbine in aero-engine under combined low and high cycle fatigue. A fatigue test on the turbine components under (HCF and LCF) loading at high temperature was carried out. They determined that the stress induced in a crack initiated is a very high through low cycle fatigue loading (thermal loading). **Wang, et al., 2016.** experimentally studied the thermal-mechanical fatigue on a single crystal nickel superalloy of a turbine blade by developing (TMF) effective test methods to investigate the deformation of the blade under (TMF) and consider it as a base of lifetime prediction. The turbine blade was heated to different temperatures from 200-1300 c^o and different times and followed by air cooling. The test was finished after 325 cycles and crack initiation was observed at suction side nearby trailing edge. In this research, the effect of load change in gas turbine on stress intensity factor will be studied

numerically and the effect of cyclic thermal load on the velocity of crack propagation will be investigated experimentally.

2 NUMERICAL ANALYSIS PROCEDURES

2.1 Model of cascade geometry

The studied model of the blade in this work represent the actual dimension of blade geometry of (37 MW) TG FIAT gas turbine of AL-Rashid power plant. To solve the case study numerically using ANSYS-FLUENT (V.17), the blade was drawing in three dimensional by (Solid Work 2012) software**.** Because of the complexity of the actual blade geometry between hub and shroud, acceptable modification to the actual geometry was done such as; Curvature of the disc was converted to straight for three blades as shown in **Fig.1** to simplify the case study, also just one blade was modeled with periodic boundary condition from suction and pressure side about it and the other two blades use for specifying the direction of the flow around the middle blade.

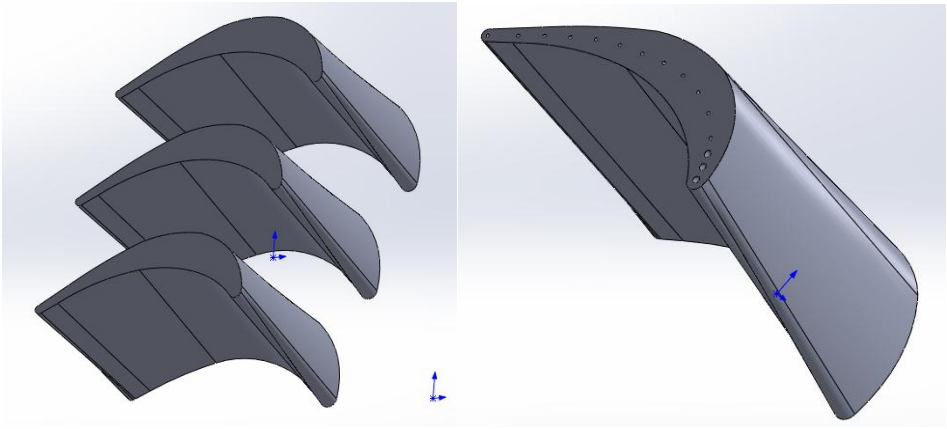

Figure 1. Model of geometry blade.

2.2 Finite volume analysis

2.2.1 grid generation and independency test

A main problem of turbine blade simulation is mesh generation that fit the boundaries of computational domain. There are many types of meshing, the mainly types are structured and unstructured meshing that resorting to them to generate grid around turbine cascade Because increase the density of cells around wall in the domain, unstructured grid are in general successful for complex geometry such turbomachinary application, for this reason the unstructured tetrahedron grid was used in this work as shown in **Fig.2**.

The method which uses to check the solution is grid independent or generates a grid has more number of cells to compare the two solutions of models as shown in **Fig.3** which clarified the number of mesh that used. Finally, for this work an average of (1443295) element is used for FLUENT and (646927) elements for static structural.

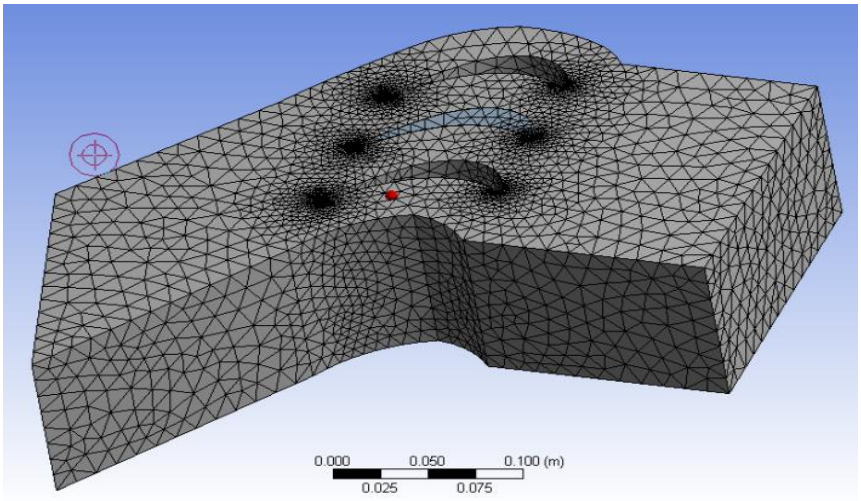

Figure 2. Unstructured tetrahedron grid**.**

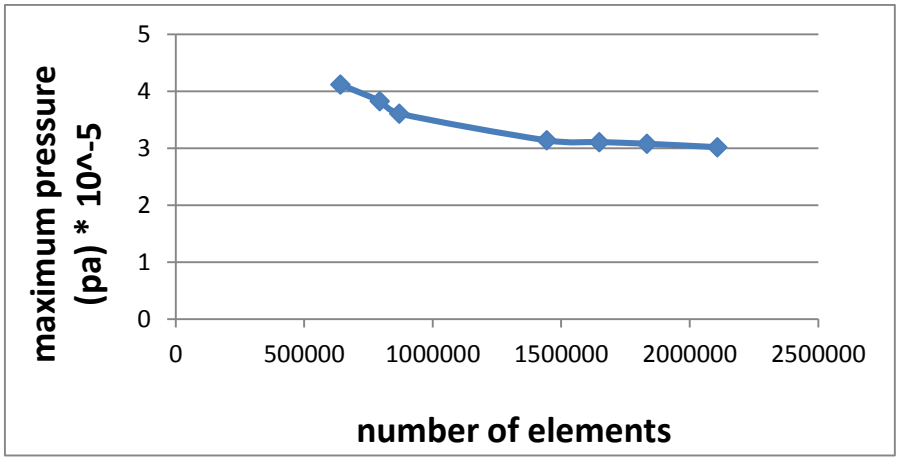

Figure 3. mesh independency test.

2.2.2 Assumption

in the present study, the working fluid was hot air and the flow characteristic were assumed to be as follows: -

1- Three dimensional

2- Incompressible flow ($Y_m = 0$).

3- Turbulent flow

4- Steady state flow $\frac{\partial \rho}{\partial t} = 0$, $\frac{\partial (\rho \bar{u})}{\partial t} = 0$

5- Single-phase flow

6- No buoyancy effect ($G_b = 0$).

2.2.3 Boundary condition

There is many type of boundary condition used in this work shown in **Fig.4** and clarified as bellow:

1- Boundary conditions were given to FLUENT to find the pressure distributions around blade were: Velocity of air inlet boundary at zone NO.1 U_{∞}= 35 m/s and the outlet boundary zone NO.2 should be placed far down from the region of interest.
2- The boundary condition gives to transient thermal to find the temperature distribution were: for surface blade convection area NO.4 the temperature varied with load, therefor used four value (550, 750, 900 and 1100) c^o and the heat transfer coefficient was 1104 $w/m^2.k$ and for the surface of cooling channel area NO.5 The temperature was 150 c^o and heat transfer coefficient was 216 $w/m^2.k$
3- Most of boundary condition given to static structural to solve the case was imported from FLUENT and transient thermal. Just gives the crack type specified in area NO.6 was semi elliptical crack and the velocity of rotation was 3000 r.p.m.

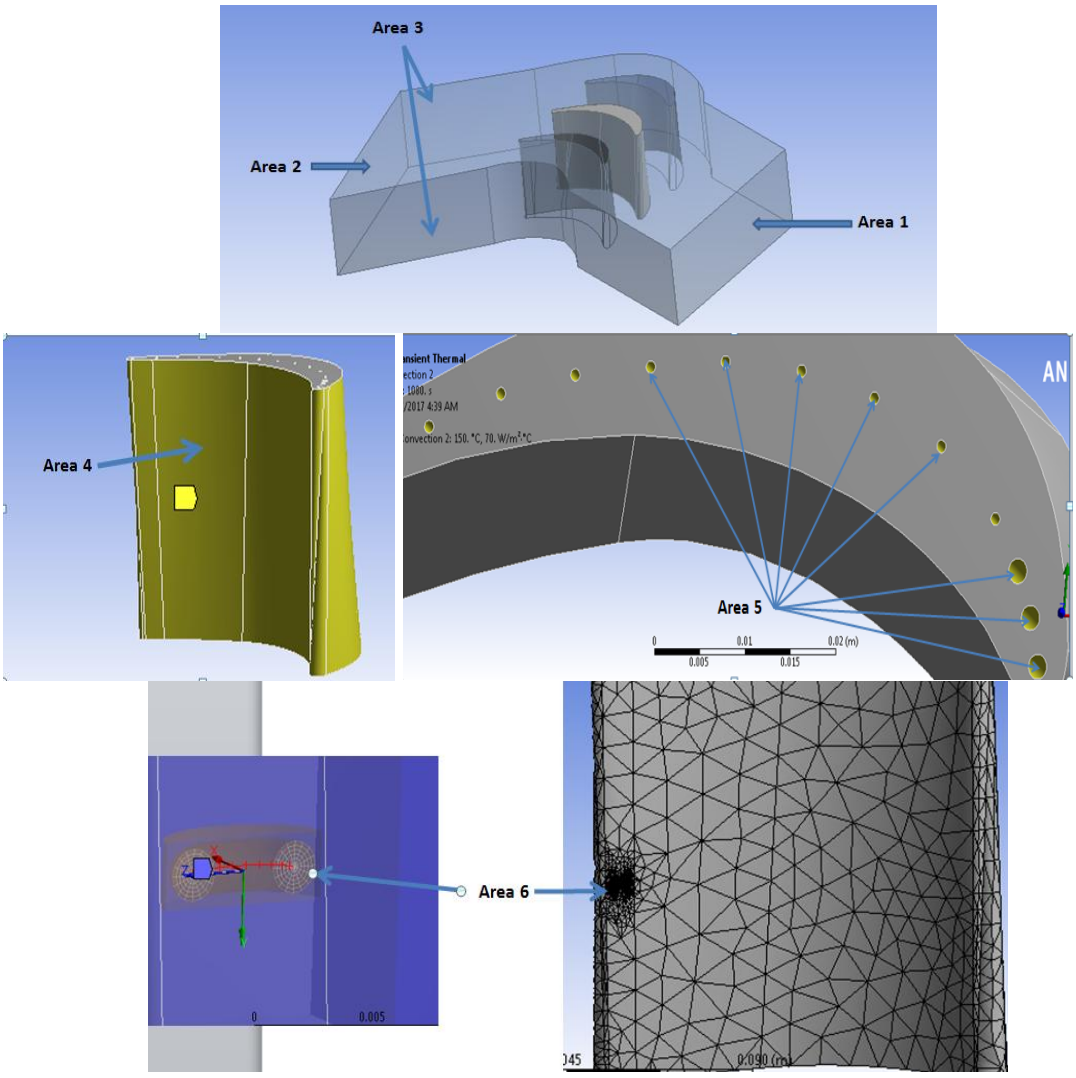

Figure 4. The boundary zone.

2.2.4 Governing equation

To simulate turbulent flow field out from the combustion chamber and flowing around turbine blade, CFD (computational fluid dynamic) Technique was used as numerical solution to solve several form of governing equation of fluid motion depended on assumption and boundary condition to obtained the pressure distribution around the turbine blade that will use to analyze the stress field that blade suffers from as shown in **Fig.5**. In this work the used governing equations were Reynolds average Navier Stokes equation (RANS) as shown below:

$$\frac{\partial \rho}{\partial t} + \frac{\partial (\rho \overline{u_i})}{\partial x_i} = 0 \tag{1}$$

$$\frac{\partial (\rho \overline{u_i})}{\partial t} + \frac{\partial}{\partial x_j}\left(\rho \bar{u}_i \bar{u}_j\right) = -\frac{\partial \bar{p}}{\partial x_i} + \frac{\partial}{\partial x_j}\left[\mu\left(\frac{\partial \bar{u}_i}{\partial x_j} + \frac{\partial \bar{u}_j}{\partial x_i} - \frac{2}{3}\delta_{ij}\frac{\partial \bar{u}_i}{\partial x_i}\right)\right] + \frac{\partial}{\partial x_j}\left(-\rho\overline{\acute{u}_i \acute{u}_j}\right) \tag{2}$$

Where $(-\rho\overline{\acute{u}_i \acute{u}_j})$ is a Reynold stress tensor which represent the effect of turbulent,**Fluent, 2013.**

To model it, Realizable $K-\varepsilon$ as turbulence model was used as shown below:

$$\frac{\partial}{\partial t}(\rho k) + \frac{\partial}{\partial x_j}(\rho k u_j) = \frac{\partial}{\partial x_j}\left[\left(\mu + \frac{\mu_t}{\sigma_k}\right)\frac{\partial k}{\partial x_j}\right] + G_k + G_b - \rho\varepsilon - Y_m + S_k \tag{3}$$

$$\frac{\partial}{\partial t}(\rho\varepsilon) + \frac{\partial}{\partial x_j}\left(\rho\varepsilon u_j\right) = \frac{\partial}{\partial x_j}\left[\left(\mu + \frac{\mu_t}{\sigma_\varepsilon}\right)\frac{\partial \varepsilon}{\partial x_j}\right]$$

$$+\rho C_1 S_\varepsilon - \rho C_2 \frac{\varepsilon^2}{k+\sqrt{v\varepsilon}} + C_{1\varepsilon}\frac{\varepsilon}{k}C_{3\varepsilon}G_b + S_\varepsilon \tag{4}$$

Where:

$$C_1 = max\left[0.43, \frac{\eta}{\eta+5}\right] \tag{5}$$

$$\eta = S\frac{k}{\varepsilon} \tag{6}$$

$$S = \sqrt{2S_{ij}S_{ij}} \tag{7}$$

$$S_{ij} = \frac{1}{2}\left(\frac{\partial u_j}{\partial x_i} + \frac{\partial u_i}{\partial x_j}\right) \tag{8}$$

G_k Represent generation of turbulence kinetic energy due to mean velocity gradient

$$G_k = \mu_t S^2 \tag{9}$$

$$\mu_t = \rho C_\mu \frac{k^2}{\varepsilon} \tag{10}$$

The model constants are:

$C_{1\varepsilon} = 1.44$, $C_2 = 1.9$, $\sigma_k = 1$, $\sigma_\varepsilon = 1.2$

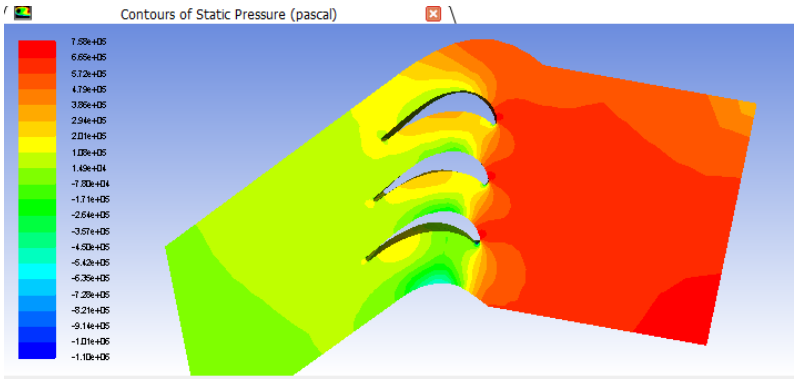

Figure 5. The pressure distribution around middle blade.

2.3 Transient thermal and structural analysis

In the real gas turbine, and according to the applied load, the turbine inlet temperature (TIT) varying with respect to the selected load, therefor the temperature distribution of the blade (max and min temp.) varying also caused significant difference temperature ΔT, which cause thermal stresses additional to centrifugal and pressure stress led to increasing crack growth. The contours of temperature distribution over the blade after three cycle (heating and cooling) and stress intensity factor were simulated used uncoupled method in ANSYS V.17, by combine pressure flow and transient temperature with structural to simulate the real condition that blade suffer from during the load change, start up and shut down as shown in **Fig.6**.

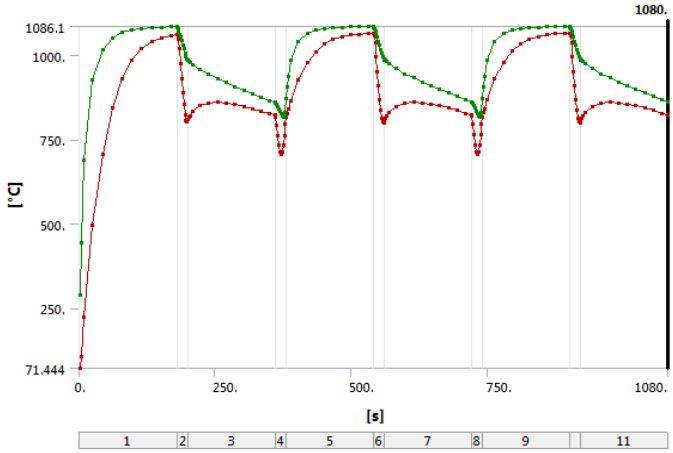

Figure 6. Cyclic thermal simulation by ANSYS.

3. EXPERIMENTAL DETAILS

Based on real and aggressive condition that gas turbine blade suffers from, an experimental rig was designed. It specially manufactured for this work as shown in **Fig.7**. The experimental work has been done using general arrangement including experimental apparatus, specimen blade, and measurement device.

Figure 7. The experimental rig

The simulation was satisfied by system includes:

Heating system: a new method is suggested depending on Oxygen-gas flame utilizing. It includes four nozzles of high temperature flame to cover the pressure side of the blade. It used an adjustable handle include valve to control the gas quantity thence control the flame temperature level. A solenoid valve has been used to open and close the stream gas channel for cyclic purpose. The heating system apparatus are shown in **Fig.8**.

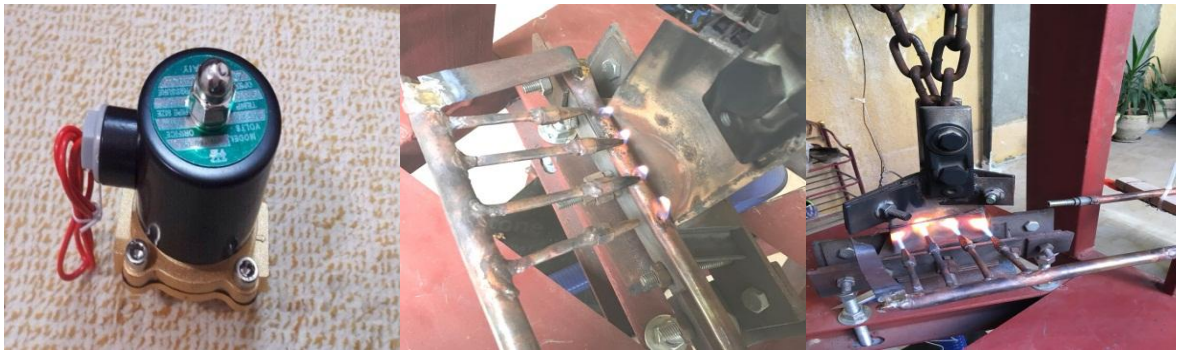

Figure 8. Heating system apparatus.

Mechanical Loading systems: in this test loading system has been used instead of centrifugal force. It assembled a frame able to bear high load, Clamping system, iron chain and hydraulic or screw jack as shown in **Fig.9**.

Figure 9. Mechanical apparatus**.**

Cooling system: To reduce the temperature of the blade to the lower limit during the test a cooling method has been used. It consists of centrifugal blower and other supplementary connection pieces connect between blower and blade as shown in **Fig.10**.

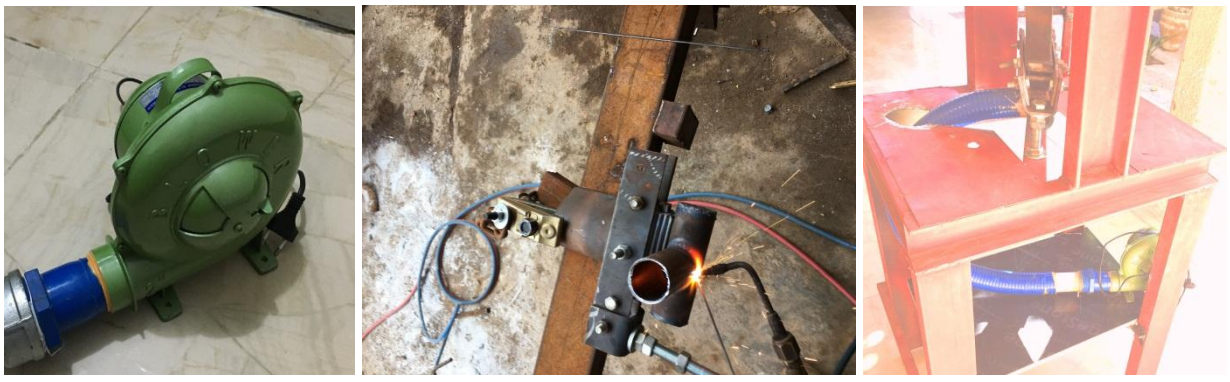

Figure 10. Cooling system apparatus.

Control system: it is the most important part in the device which responsible on the cycling behavior of the thermal load supplied on the turbine blade (heating and cooling). it including control panel and all other components electronic element. The control system takes the input signal from the thermocouple then treated it and sending signal to the heating or cooling system (depended on temperature) to makes it on/off based on Arduino language software (ID) as shown in **Fig.11**.

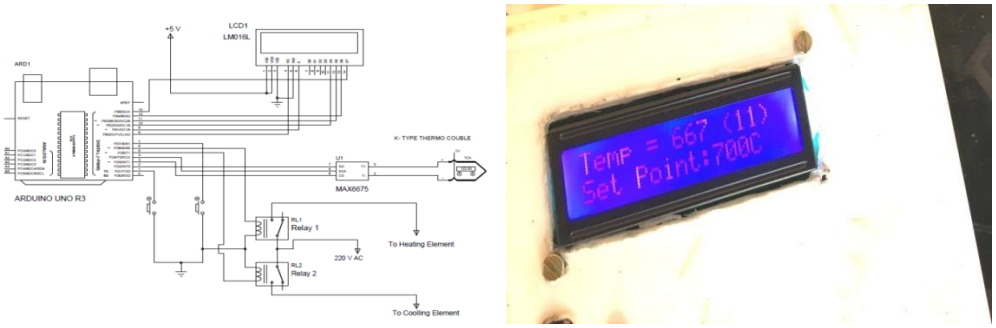

Figure 11. Control system layout.

Measuring instrument and monitoring systems: Fig.12 clarifies measuring and monitoring instruments which were used in this test. It involves thermocouple type K which was fixed on the back of blade surface, digital vernier caliper with 0.01 mm resolution which was utilized to measure the length of the crack, Load cell type with weight indicator which was used to measure the load, software package which was used to count the number of cycles and two lenses used to monitor the surface of blade to find defects and crack growth. One of them has zoom ability around (2-20 X) and the other has up to (45 X).

Figure 12. Measurement and monitoring instruments.

The specimen: The specimen used in this test was an actual blade from first stage rotating blade of (37) MW (TG 20) FIAT gas turbine as shown in **Fig.13** before the test.

Figure 12. The specimen before test.

3.1 Test procedure

The experimental work was carry out based on the rig operation steps as described in several steps as mention below:

1- Give power supply from source to control panel.

2- Set the minimum and maximum temperature of cycle.

3- Open the gas and oxygen bottle and adjust the regulator valve (adjustable handle) to get the best flame

4- Open the gate of blower to get maximum flow rate of cooling air.

5- Start burn the nozzle of flame.

6- Operate the power supply of heating system (solenoid valve) and cooling system (blower) from control panel itself.

7- Record the time of each cycle and the number of cycle.

8- After each 5 cycle stopped the device and measure the length of crack.

These steps repeated respectively after each 5 cycles.

4 THE RESULTS

4.1 numerical results

The numerical results were investigated the stress intensity factor (K) and thermal stress numerically for four real gas turbine inlet temperature (TIT) for two cases, start-up, and shutdown (no load, 50% load, 75% load and full load). In all case the peak stress of the blade occurs at the trailing bottom edge near where failures occur, as below details of four cases clarified:

Case one: For case one the TIT was 550 C^o that mean the turbine in idle mode (full speeds no load). **Fig.13** clarifies the contours of transient temperature after three cycles 720 and 900 second. In this case noted that max temperature (537 C^o) and min temperature (331 C^o) between start-up and shutdown. This difference cause thermal stress affected on the crack growth in all direction. **Fig.14** shown the total stresses field depended on pressure load, centrifugal force and temperature gradient. **Fig.15** clarify the stress intensity factor for crack carry out by ANSYS on surface blade after zoom it, in two direction of crack and noted that max K was (6.37 Mpa.$\sqrt{m}$) happened in the middle of crack in the direction of cooled channels and at the left side in the direction of tip trailing edge that led to growth the crack in this direction which consider the same direction that happened in the experimental test.

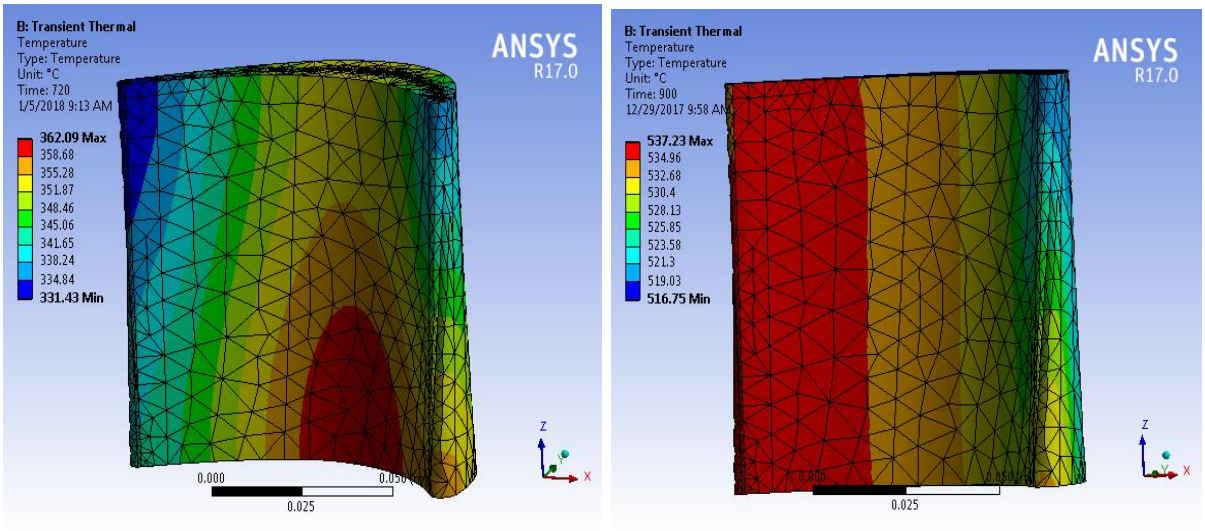

Temp. Distribution after 720 s Temp. Distribution after 900 s

Figure 13. Temp. Distribution.

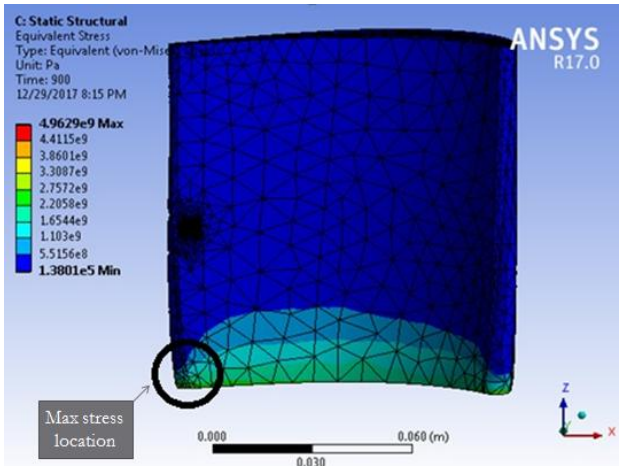

Figure 14. Stress distribution.

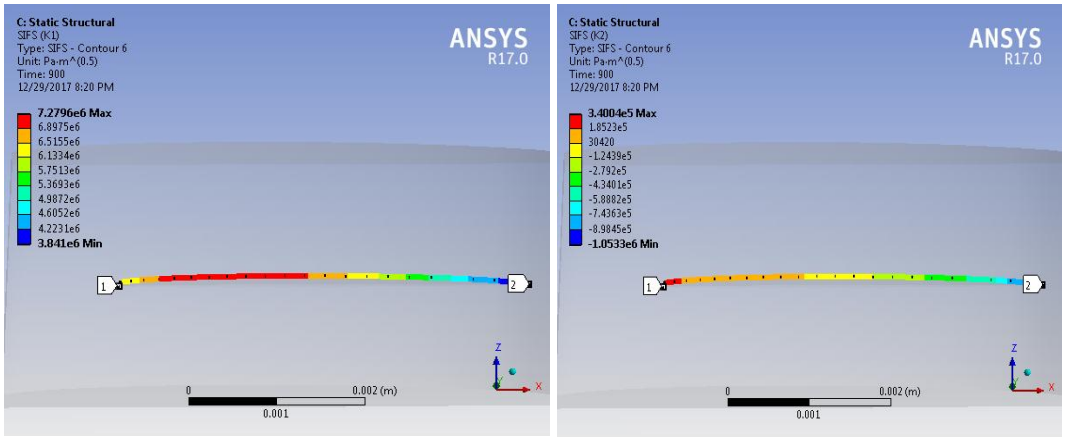

K1 K2

Figure 15. Stress intensity factors for crack after zoom it

The other three cases are abbreviations in table below. It shows the TIT, max and min temperature and max stress intensity factor with the number of figure which clarified it.

NO. of case	TIT (C°)	T_{max} (°C)	T_{min} (°C)	Temp. distribution figure	*T*hermal stress figure	K_{max} (mpa.$\sqrt{m}$)
two	750	730	426	**Fig.16**	**Fig.17**	9.5 **Fig.18**
three	900	876	497	**Fig.19**	**Fig.20**	11.16 **Fig.21**
four	1100	1069	593	**Fig.22**	**Fig.23**	13.38 **Fig.24**

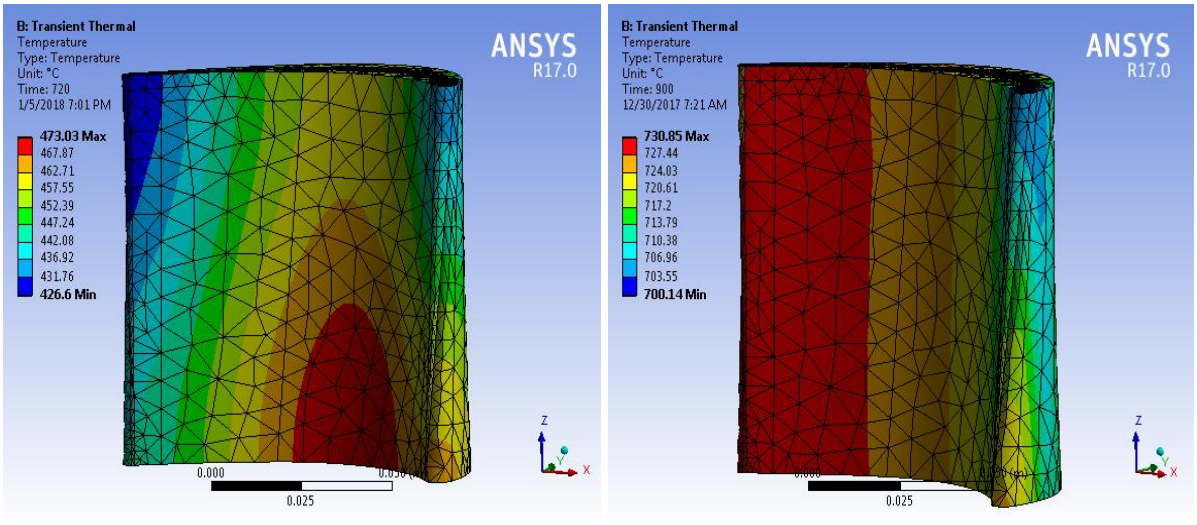

Temp. Distribution after 720 s Temp. Distribution after 900 s

Figure 16

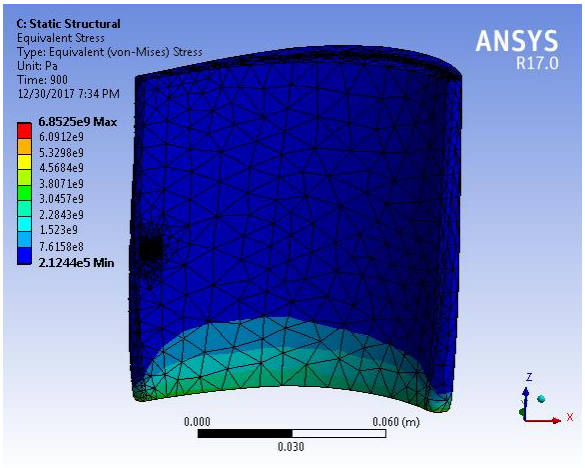

Figure 17. Stress distribution.

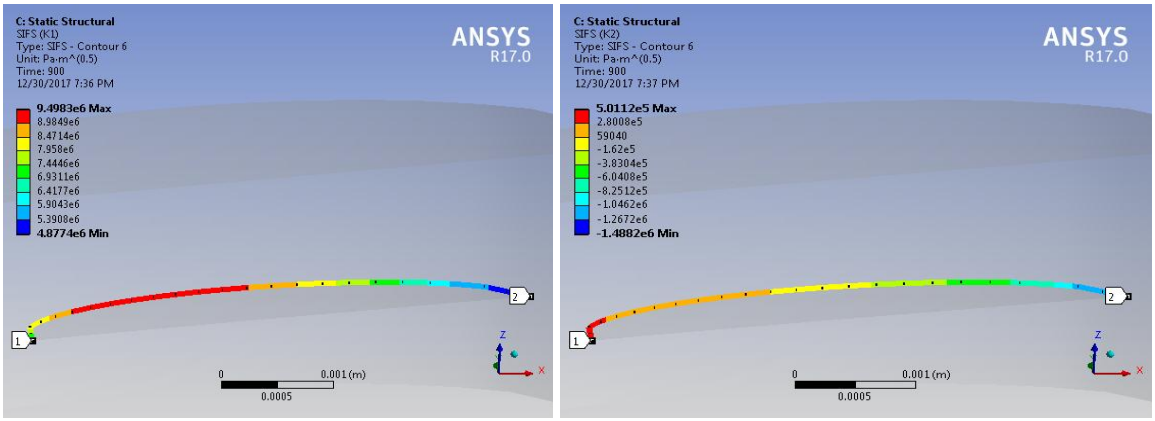

K1 K2

Figure 18. Stress intensity factor for crack after zoom it.

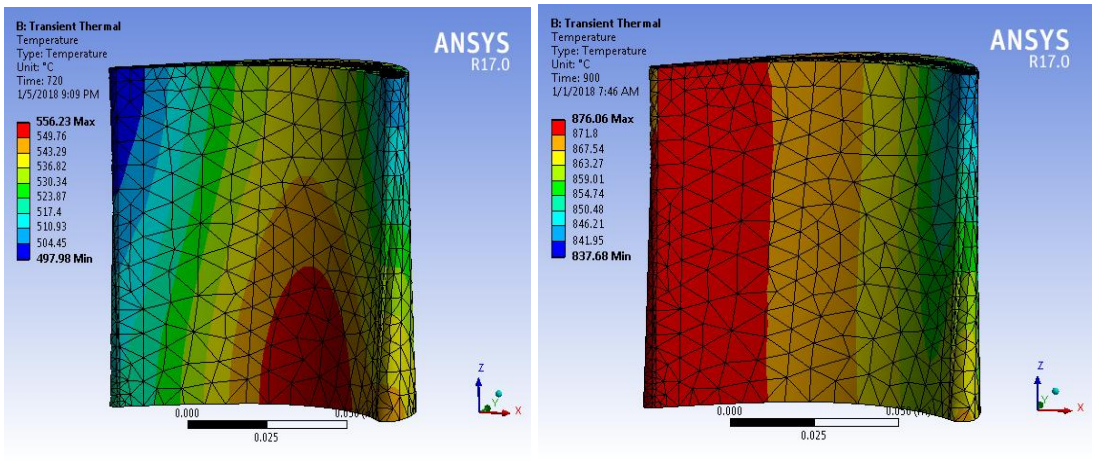

Temp. Distribution after 720 s Temp. Distribution after 900 s

Figure 19

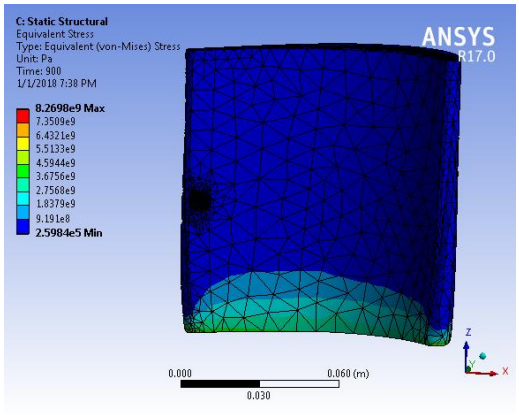

Figure 20. Stress distribution.

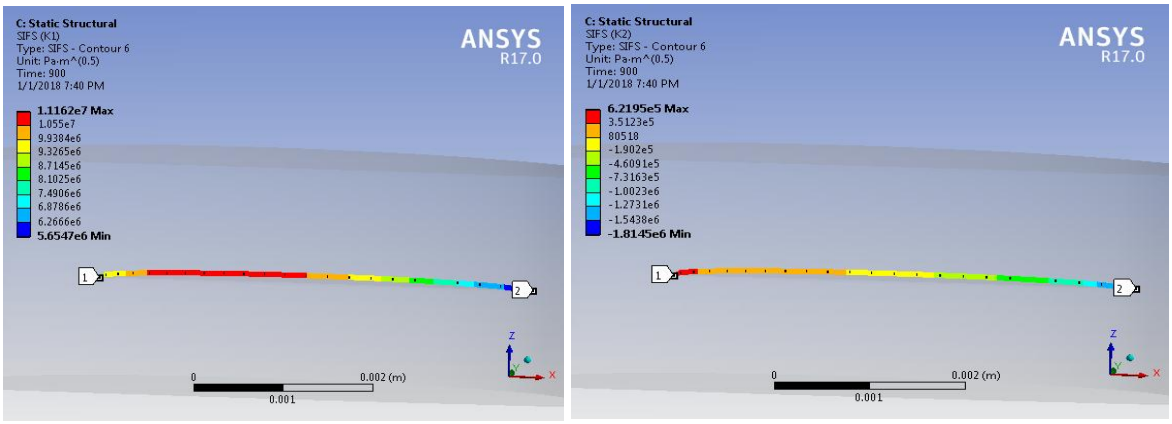

K1 K2

Figure 21. Stress intensity factor for crack after zoom it.

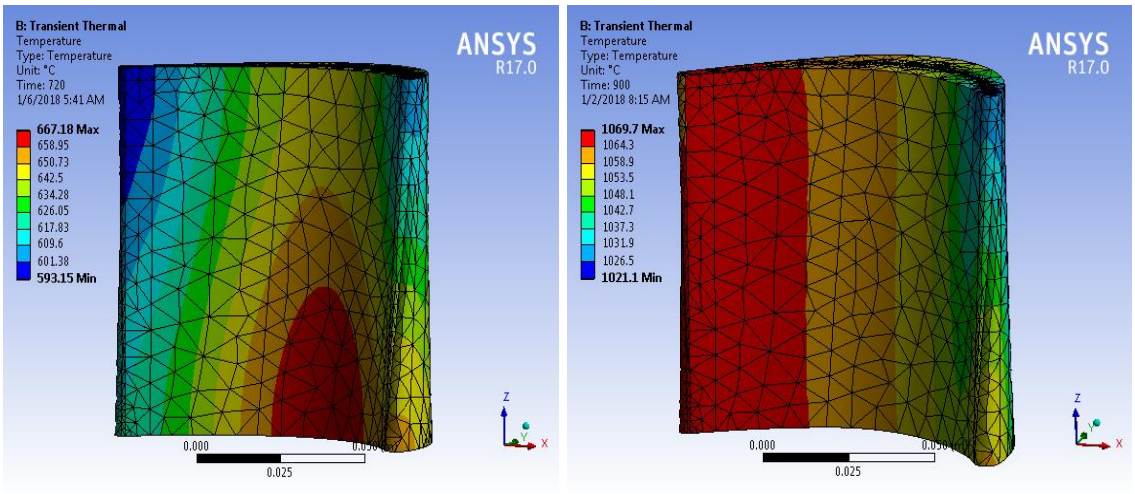

Temp. Distribution after 720 s Temp. Distribution after 900 s

Figure 22. Temp. Distribution.

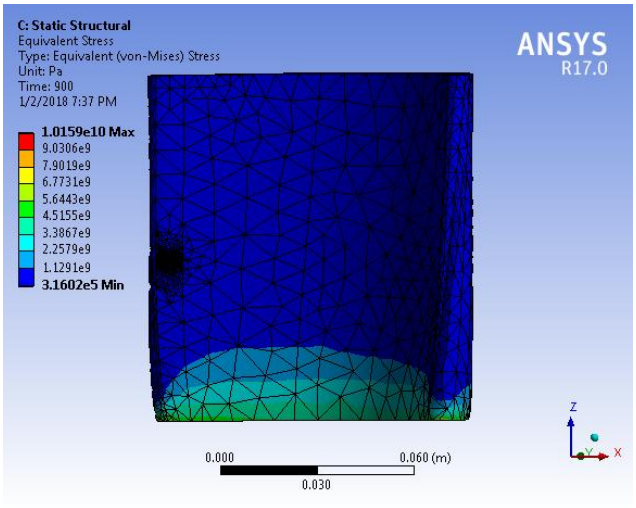

Figure 23. Stress distribution.

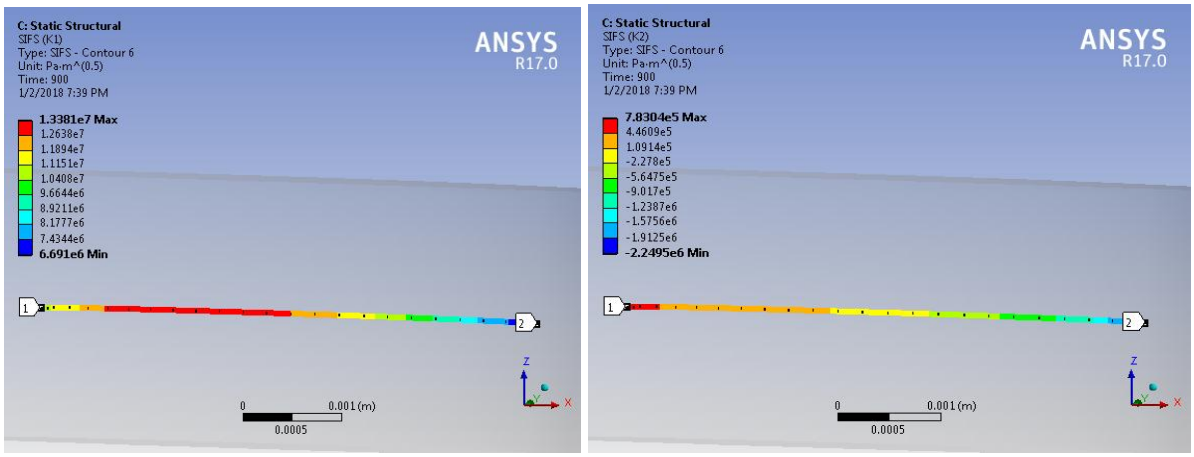

K1 K2

Figure 24. Stress intensity factors for crack after zoom it.

4.2 Experimental results

The crack length was measured at various position of the blade throughout intervals of 460 cycles as shown in **Fig.25**. In these test Δσ is the main parameter to define the cycle that affected on stress intensity factor K. The aim is to found the crack growth rate (da/dn) for two type of crack: horizontal and inclined crack with angle α, which depended upon ΔK that varies with the stress value and the crack propagation modes as clarify in equations below, **Socie and Marquis, 2000**:

$$\Delta\sigma = \sigma_{max} - \sigma_{min} \quad (11)$$

$$K_I = \frac{\sigma\sqrt{\pi a}}{2}\{(1+\lambda) + (1-\lambda)cos2\alpha\} \quad (12)$$

$$K_{II} = \frac{\sigma\sqrt{\pi a}}{2}\{(1-\lambda)sin2\alpha\} \quad (13)$$

For horizontal crack, α equal to zero therefor the stress intensity factor become:

$$\Delta K = \beta \Delta \sigma \sqrt{\pi a} \quad (14)$$

Where:

a: crack length (m).

σ_{min}: minimum stress in cycle (pa).

σ_{max}: maximum stress in cycle (pa).

β: the geometry factor = crack length / width of the specimen

λ: biaxial principle stress ration (σ_{II} / σ_I), in this test equal to (0.64)

α: the angle of inclined crack with the horizontal axis (for middle crack = 73°) as shown in **Fig.26**

Then the crack growth rate can be calculated from Paris equation as:

$$\frac{da}{dn} = c_p(\Delta K)^{m_p} \quad (15)$$

(Schütz 1989)

To find the parameter (c_p and m_p), A functional form can be established by fitting a curve of test data (ΔK vs. $\frac{\Delta a}{\Delta N}$) for two crack at trailing edge (horizontal crack) and at the middle of blade (inclined blade) as shown in **Fig.27** (a, b and c)

It can be noted that the rate equation for trailing edge crack is $\frac{da}{dn} = 4.8 * 10^{-8}(\Delta K)^{3.15}$ and for middle crack is; for mode I $\frac{da}{dn} = 9.26 * 10^{-10}(\Delta K)^{4.17}$ and for mode II $\frac{da}{dn} = 6.45 * 10^{-5}(\Delta K)^{3.65}$ these are all the information which can be extracted directly from the experimental test to find the form of rate equation. It can be noted that the rate equation for each crack is different from other, as a result of the temperature of crack location area and the thickness of the blade in this location.

Also From the plotted figure it can be noticed that, the crack may stop for some cycle and has irregular crack growth. This possibly is owing to the microstructure of the material and the crack reaches the grain boundary or it merges with the microcrack because of the irregularity of material. This factors leads to a jump in the a-N curves and affect another results.

Figure 25. The failure blade after 460 cycles.

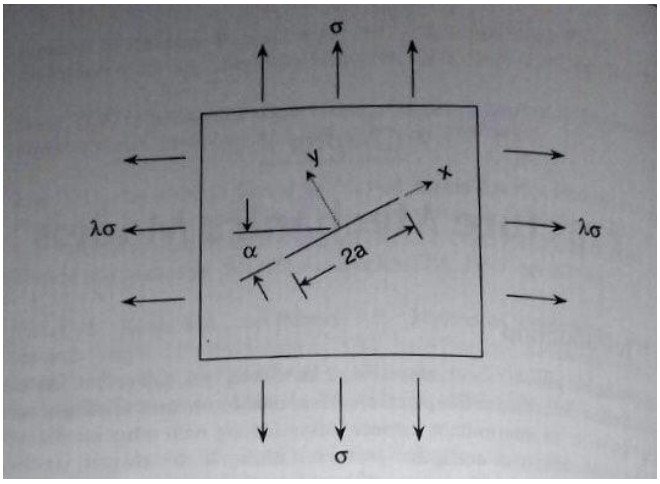

Figure 26. Clarified α and λ **(Socie and Marquis, 2000)**.

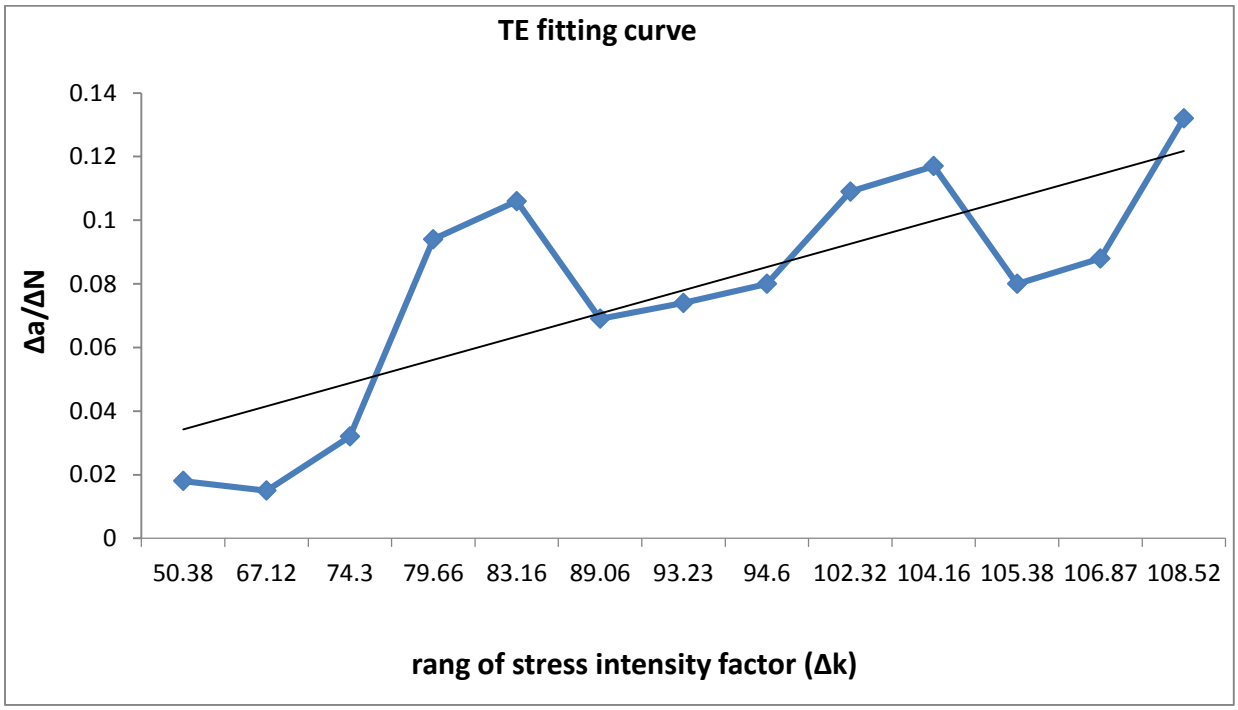

Figure 27a. Δk – Δa/ΔN curve fitting for trailing edge crack.

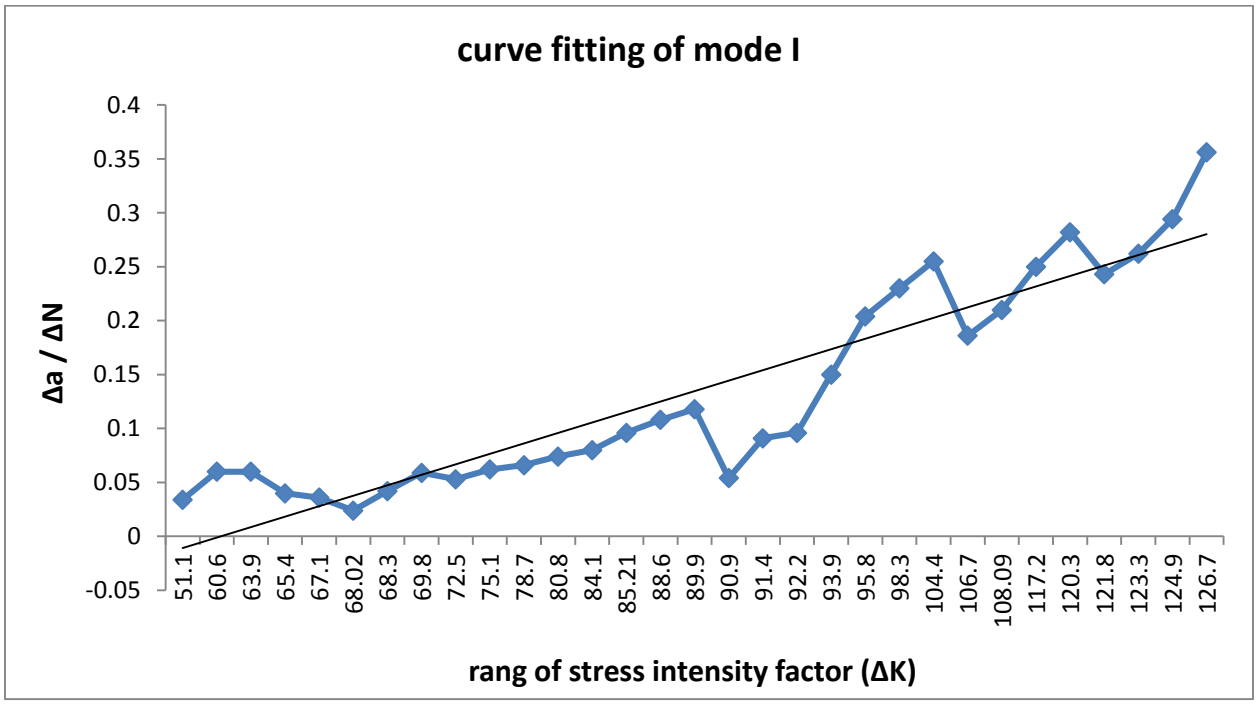

Figure 27b. Δk – Δa/ΔN curve fitting for mode I in middle crack.

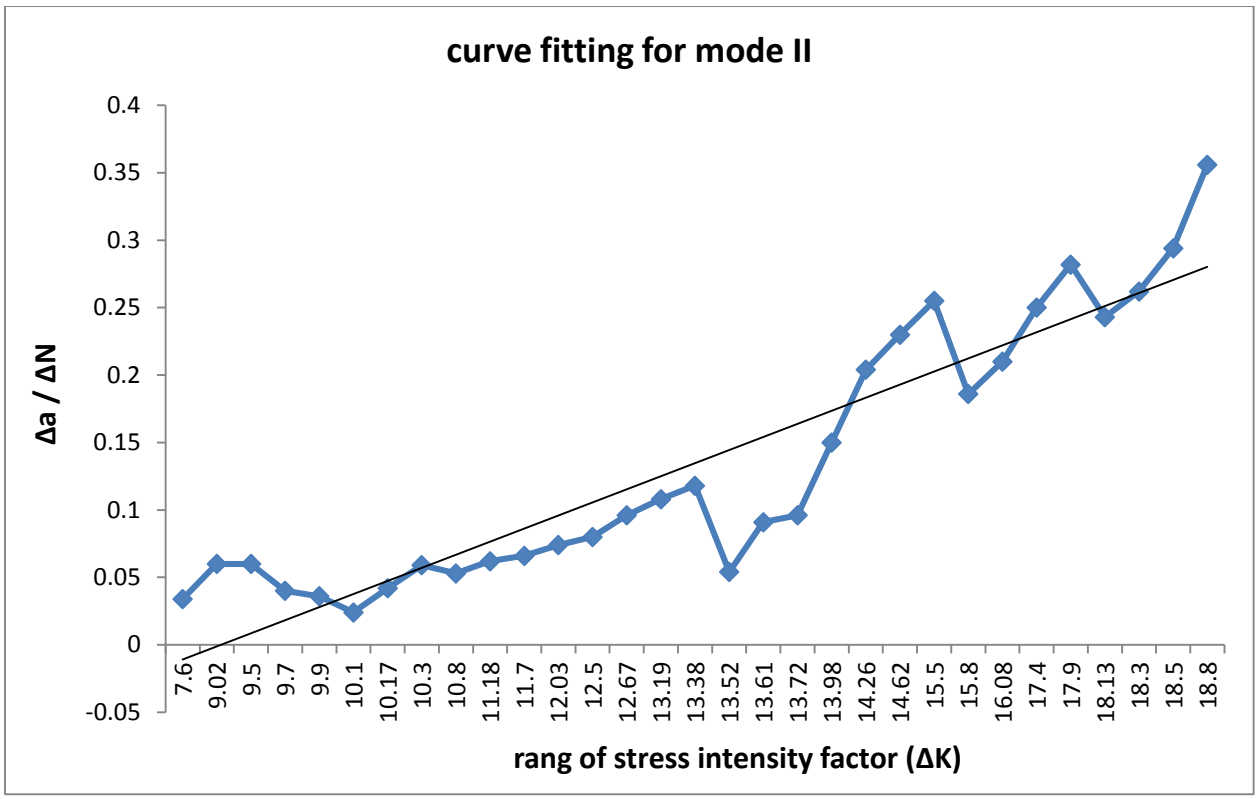

Figure 27c. Δk – Δa/ΔN curve fitting for mode II in middle crack.

CONCLUSION

As a result of high temperature, start-up, shutdown and load change, a cyclic thermal load is induced in the gas turbine blade. Then as a result of cyclic thermal load, the stress intensity factor was varying from load to load, and the velocity of crack growth is varying depending on the location and the inclined of crack in blade surface. These parameters of crack directly affect the lifetime of the blade. Using Paris equation, it can estimate the number of cycles remained before failure happened and satisfied which crack more affected on a lifetime of blade, and then save the healthy blade from destroyed by failure blade. From the numerical simulation, it can be noted that Increasing the load, much-repeated start-up, shut-down and load change on turbine engine lead to increase the chance of blade failure due to increasing stress intensity factor and cyclic thermal. It can be noted also that the maximum stress is occurring at the root of the trailing edge side from turbine blade which makes it the weakness region to initiate the crack. From the experimental results, it can be noted that the middle crack has inclined growth as a result of the mixed mode of crack growth mode I and mode II due to the mechanical and thermal stress effect (multiaxial fatigue). It can also be noted due to the horizontal and the longitudinal temperature gradient, ΔK_{II} is more effective on the rate of crack growth compared with ΔK_I at the inclined crack as clarified from rate equation of inclined crack. From the test, it can be noted that the crack has a high velocity of growth after 350 cycles which can be considered the failure happened. It can also conclude in two main points depended on the comparison between velocity of crack propagation that:

1- The trailing edge crack has the higher rate propagation from the other crack which growth in mode I behavior (horizontal growth) due to its location which has higher temperature, less thickness and higher stress.
2- The middle crack has the higher rate propagation from all other crack due to the effect of mixed mode of crack growth behavior mode I and mode II.

REFRENCE

- Bhaumik, S. K., M. Sujata, M. A. Venkataswamy and M. A. Parameswara ,2006. *Failure of a low pressure turbine rotor blade of an aeroengine*. Engineering Failure Analysis **13**(8): 1202-1219.

- Fluent, A. 2013. *ANSYS Fluent Theory Guide*.

- Kim, H. 2009. *Study of the fracture of the last stage blade in an aircraft gas turbine*. Engineering Failure Analysis **16**(7): 2318-2324.

- L. Jacobsson, C. P., S. Melin , 2004. *Experimental methods for thermo mechanical fatigue in gas turbine materials*. Proceedings of The 15th European Conference on Fracture, Stockholm, Sweden.

- Park, M., Y.-H. Hwang, Y.-S. Choi and T.-G. Kim , 2002. *Analysis of a J69-T-25 engine turbine blade fracture.* Engineering Failure Analysis **9**(5): 593-601.

- Schütz, W. 1989. *The practical use of fracture mechanics. von David Broek, Kluwer Academic Publishers, Dordrecht*, Boston, London, 1988, 522 Seiten, rd. 120 Abb., rd. 40 Tab., Format 16 × 240 mm, Halbl." Materialwissenschaft und Werkstofftechnik **20**(5): A50-A50.

- Socie, D. and G. Marquis 2000. *Multiaxial Fatigue, Society of Automotive Engineers.*

- T. Jiang, R. D. X., G.Y. Liu, W.F. Zhang 2003. *Fracture failure analysis for turbine blades of II stage*. J. Mater. Eng(z1. 162–165).

- V.Veeraragavan ,2012. *Effect Of Temperature Distribution In 10c4/60c50 Gas Turbine Blade Model Using Finite Element Analysis*. International Journal of Engineering Research & Technology (IJERT) **1**.

- Wang, R., K. Jiang, F. Jing and D. Hu ,2016. *Thermomechanical fatigue failure investigation on a single crystal nickel superalloy turbine blade*. Engineering Failure Analysis **66**: 284-295.

- Wang, R., F. Jing and D. Hu ,2013. *In-phase thermal–mechanical fatigue investigation on hollow single crystal turbine blades.* Chinese Journal of Aeronautics **26**(6): 1409-1414.

- Z. Zhuang, W. and N. S. Swansson ,1998. *Thermo-Mechanical Fatigue Life Prediction: A Critical Review.*

NOMENCLATURE

a	crack length, m
c_p , m_p	parameter deepened on material
k	stress intensity factor, Mpa.√m
N	number of cycle
$\bar{u}_i$	mean component of velocity, m/s
$\acute{u}_i$	fluctuating component of velocity, m/s
$\bar{P}$	average pressure, pa
ΔT	temperature difference, c^o
x_i	X direction
x_j	Y direction

Greek letters

σ_{min}	minimum stress in cycle, pa
σ_{max}	maximum stress in cycle, pa
β	the geometry factor
λ	biaxial stress ratio
α	the angle of inclined crack with the horizontal axis